Ilorin Journal of Science
Volume 7, Number 1, 2020, pp. 66 – 82 (Printed in Nigeria)
ISSN: 2408 – 4840 © 2020 Faculty of Physical Sciences, University of Ilorin
https://doi.org/10.54908/iljs.2020.07.01.005

ILORIN
JOURNAL OF SCIENCE

**ILJS-17-006**

# Spatio-Temporal Variation of Download Longwave Radiation over Nigeria.

**Fadina*, S. A, Fakoya, A. A., Akoshile, C. O. and Ajibola, T. B.**

Department of Physics, University of Ilorin, Ilorin, Nigeria.

## Abstract

This study seeks to investigate the spatial and temporal variation of LWD over Nigeria. This was achieved with the aid of LWD spatial maps and variograms, generated using FLDAS LWD product for the period 2002 – 2009. The FLDAS LWD data was validated using in-situ LWD measurement for the period 1992 – 2005 obtained from the BSRN site at the University of Ilorin, Nigeria. A high correlation of 0.94 exists between the two datasets with MAE, MBE and RMSE of 4.00, 0.2155 and 4.84, respectively. The monthly averages across the study area show LWD is higher during the rainy season with a double maximum occurring in May and August, compared to the dry season with the lowest LWD occurring in January. A more uniform spatial variation during the rainy season compared to the dry season has indicated by the low STD, dissimilarity values and uniform colour of radiation maps. The high value of LWD during the rainy season may be attributed to the high moisture content of the atmosphere, this study reaffirms water vapour as a major source of LWD. The LWD map developed in this study is useful for identifying spatial patterns that are not detectable from in-situ LWD measurements.

**Key words**: Downward Longwave Radiation, Radiation Map, Water Vapour, Monthly Variation, Variogram.

## 1. Introduction

Downward longwave radiation (LWD) which is an important component of the earth's radiation budget is a measure of the longwave radiation incident on the earth's surface, originating from the earth's atmosphere. Atmospheric downward longwave radiation is measured directly using a pyrgeometer or estimated from satellite observations and other weather parameters such as; temperature, surface water vapour pressure, relative humidity etc. LWD is emitted when atmospheric particles such as carbon dioxide, ozone molecules and cloud water droplets etc. absorb solar radiation along with the absorption of upward thermal radiation emitted by the surface (Idso and Jackson 1969; Mölders *et al*., 2008), hence the variation of LWD is influenced by the presence of greenhouse gases in the atmosphere.

*Corresponding Author: Fadina, A. S.

Email: fadinaadeolu@gmail.com

In principle, LWD substantially influences net radiation and evapotranspiration, which are critical factors in understanding surface energy distribution, hydrological cycles and water resource management at various scales (Ryu *et al*., 2008). LWD plays a vital role in studying the origin of climate change and is perhaps the most fundamental for understanding the impact of increasing carbondioxide ($CO_2$) and other greenhouse gases (GHG) on climate (Iacono *et al*., 2008) but is also considered to be the most poorly quantified from observations (Trenberth and Fasullo, 2012; Trenberth *et al.*, 2009) compared to other components of the radiation budget. LWD is being measured at a few weather stations due to the cost of pyrgeometers and the difficulty in maintenance and other challenges encountered in the direct measurement of LWD. In-situ observations have been made available through some internationally coordinated monitoring activities, such as the World Climate Research Programme (WCRP) Baseline Surface Radiation Network (BSRN) (Ohmura *et al.*, 1998), and the Global Energy and Water Cycle Experiment (GEWEX) Coordinated Energy and water cycle Observations Project (CEOP) (Koike, 2004; Lawford *et al.*, 2006), providing long-term continuous measurements of LWD at globally distributed sites, in particular at the BSRN sites while other remote-sensing products of LWD are also available.

Different studies have proposed several empirical models for estimating LWD using commonly measured weather parameters, the most commonly used observations are air temperature and vapour pressure (e.g. Abramowitz *et al*., 2012; Ångström, 1918; Brunt, 1932; Idso and Jackson, 1969; Swinbank, 1963). Wang and Liang (2009) used the Brunt (1932) and Brutsaert (1975) model to estimate global atmospheric LWD under both clear and cloudy conditions, using surface incident shortwave radiation, air temperature, relative humidity date from 1996 to 2007 at 36 globally distributed sites, operated by the Surface Radiation Budget Network (SURFRAD), AmeriFlux, and AsiaFlux Projects for six different land cover types. Their result shows that both models can be applied to most of the Earth's land surfaces and increase in LWD is strongly correlated to increases in air temperature, atmospheric water vapour, and $CO_2$ concentration. Sur *et al*. (2014) generated a map of LWD for North-East Asia to study the Spatio-temporal variation of LWD for Northeast Asia, using satellite dataset from the MODIS-based LWD algorithm. Their result indicates that LWD can be estimated with remote sensing-based T and *e* with reasonable accuracy, whereas a ground measurement of LWD was not possible (Sur *et al.*, 2014).

In this study, the Spatio-temporal variation of LWD over Nigeria was investigated by generating LWD radiation maps for Nigeria and variogram using Famine Early Warning Systems Network (FEWS NET) Land Data Assimilation System (FLDAS) (McNally *et al.,* 2017) LWD product.

## 2. Materials and Methods

### 2.1 Study site and Ground Measurement Data

The Baseline Surface Radiation Network (BSRN) site at the University of Ilorin (8.4799 °N, 4.5418 °E), Nigeria was selected for the validation of FLDAS LWD dataset. BSRN is a project of the Data and Assessments Panel from the Global Energy and Water Cycle Experiment (GEWEX) under the umbrella of the World Climate Research Programme (WCRP). BSRN sites are located at different locations across the globe. The site at the University of Ilorin, Nigeria, was part of the network until 2005. The BSRN data are of primary importance in supporting the validation and confirmation of remote-sensed and model estimates of the measured quantities. BSRN LWD data (over the period 1992 - 2005 with a time resolution of 1 to 3 minutes) measured with an Eppley Precision Infrared Pyrgeometer were downloaded from the BSRN Pangea portal (https://www.pangaea.de)

### 2.2 Famine Early Warning Systems Network (FEWS NET) Land Data Assimilation System (FLDAS)

The Famine Early Warning Systems Network (FEWS NET) Land Data Assimilation System (FLDAS) produces multi-model and multi-forcing estimates of hydro-climate conditions such as soil moisture, evapotranspiration, and runoff using rainfall and other meteorological inputs (temperature, humidity, radiation, and wind) (McNally *et al.,* 2017). The FLDAS system was created under a NASA Applied Sciences Program Water Resources grant as a collaboration between the U.S. Geological Survey (USGS) Earth Resources Observation and Science (EROS) Center, NASA Goddard Space Flight Center (GSFC), and the University of California Santa Barbara (UCSB) Climate Hazards Group (CHG) (McNally *et al.,* 2017). FLDAS models use FEWS NET specific rainfall products and other meteorological inputs such as; temperature, humidity, radiation, and wind. To generate low-latency products FLDAS uses NOAA Global Data Assimilation System (GDAS) 3-hourly meteorological inputs available from 2001-present at 1-day latency. For a longer historical record, FLDAS

uses NASA's Modern Era Reanalysis for Research and Applications version 2 (MERRA-2) (1979-present) 1-hourly products with a two-week latency. The time series area-averaged LWD data from FLDAS model for the period 2002 – 2009 with a time resolution of 1 month for each geographical coordinates corresponding to the grid intersects of the study area (figure 1.) where downloaded from "NASA earthdata" portal (https://giovanni.gsfc.nasa.gov).

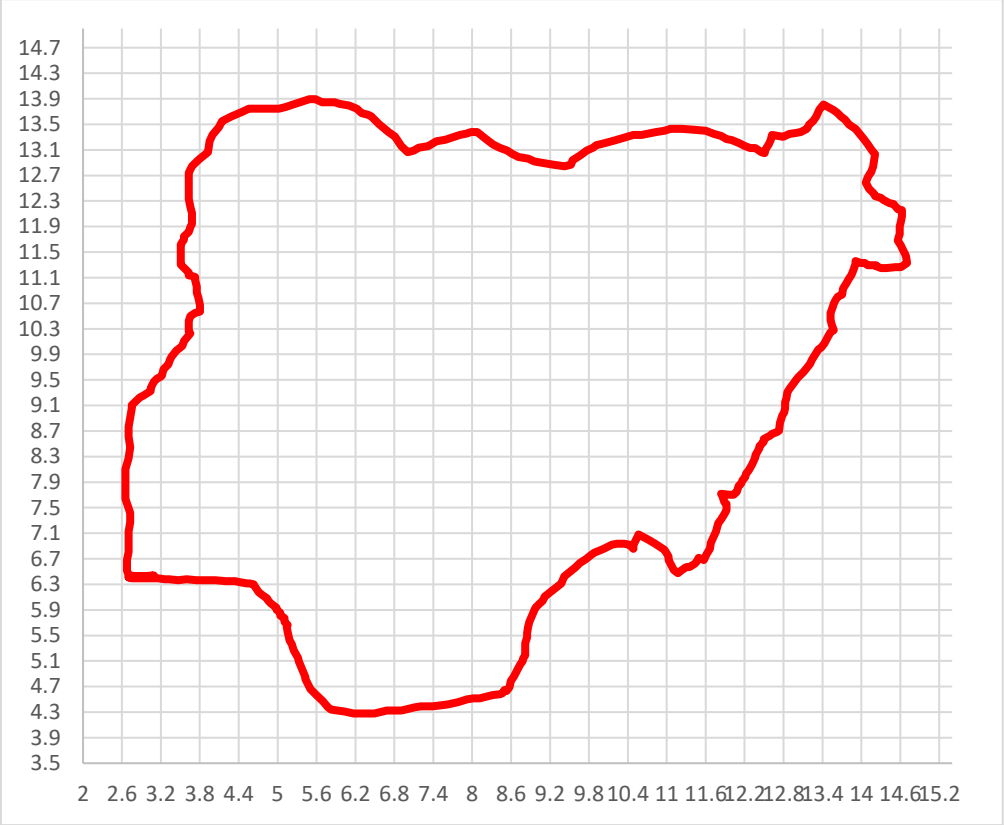


**Figure 1:** A gridded map of Nigeria.

### 2.3 Data Processing

Data processing was required to transform the data into the appropriate resolution, the BSRN LWD observations originally in 1 – 3 minutes time resolution was resampled into monthly resolution. The time series area-averaged LWD data over bounding box coordinates 4.56°E, 8.52°N, 4.57°E, 8.53°N was used for the validation of FLDAS LWD product. To determine the overall monthly variation, compensate for missing data and outliers present in a particular year, the FLDAS LWD data and BSRN LWD data were processed to obtain the multi-year monthly average for the two datasets. As validation, the degree of deviation between the two datasets was evaluated using the root mean square error (RMSE), Mean Absolute Error (MAE), Mean Bias Error (MBE) and Pearson correlation coefficient. RMSE sums up the

magnitude of error in prediction for various times into a single measure predictive power, MAE measure gives an idea of the magnitude of the error, but no idea of the direction while MBE gives an idea of the magnitude and direction of the error.

$$RMSE = \{[\sum(L_f - L_s)]/n\}^{1/2}, \quad (1)$$

$$MAE = [\sum|L_f - L_s|]/n, \quad (2)$$

$$MBE = [\sum(L_f - L_s)]/n, \quad (3)$$

where, $L_s$ is the BSRN LWD data, $L_f$ is the FLDAS LWD data and n is the number of observations.

**2.4 Variogram**

The variogram is commonly used to describe the spatial correlation of observations in geostatistics, predicated on the idea that spatial relationship between two sample points does not depend on their actual geographical location, but rather on their relative position. Variogram illustrates where a significant correlation in a sample space disintegrates into randomness when the variance terms of an in-situ ordered set are plotted against the variance of the set and the lower limits of its 99% and 95% confidence ranges (Wackernagel, 2003). The sample pairs are calculated by measuring the square difference between values and the correlation between two regionalized variable pairs is dissimilarity. Dissimilarity ($\gamma_{\propto\beta}$) between pairs of data values, $z_{\propto}$ and $z_{\beta}$ say, located at points $x_{\propto}$ and $x_{\beta}$ in a spatial domain D is given as:

$$\gamma_{\propto\beta} = \frac{(z_{\propto} - z_{\beta})^2}{2}, \quad (4)$$

we let the $\gamma_{\propto\beta}$ depend on the spacing and the orientation of the point pair described by the vector **h** (Wackernagel, 2003)

$$\gamma(\boldsymbol{h}) = \frac{1}{2}(z(x_{\propto} + h) - z(x_{\propto}))^2 . \quad (5)$$

A plot of the dissimilarities ($\gamma_{\propto\beta}$) against the absolute spatial separation (**h**) is called the variogram cloud, which is divided into various groups according to separation and orientation in space; the mean dissimilarities in each group form the order of values of variogram; the average dissimilarity between values increases when the spacing between the pairs of sample

points is increased. This is because the sample points close to each other in a spatial space tend to be alike. There is no spatial arrangement in the data when the mean dissimilarity of values is constant for the spacing **h**. In comparison, a negative or positive incline of the variogram at the origin indicates a structure. A sudden slope transition reveals the passage to another spatial value system. The variogram function is fitted to the series of average dissimilarities, which distinguishes both the behaviour at the origin and large distances (Figure 2 & 3). Anomalies, inhomogeneities can be detected by looking at high dissimilarities at short distances. The variogram was generated with a software called "Field Pro" using the time series area-averaged FLDAS LWD dataset for each month.

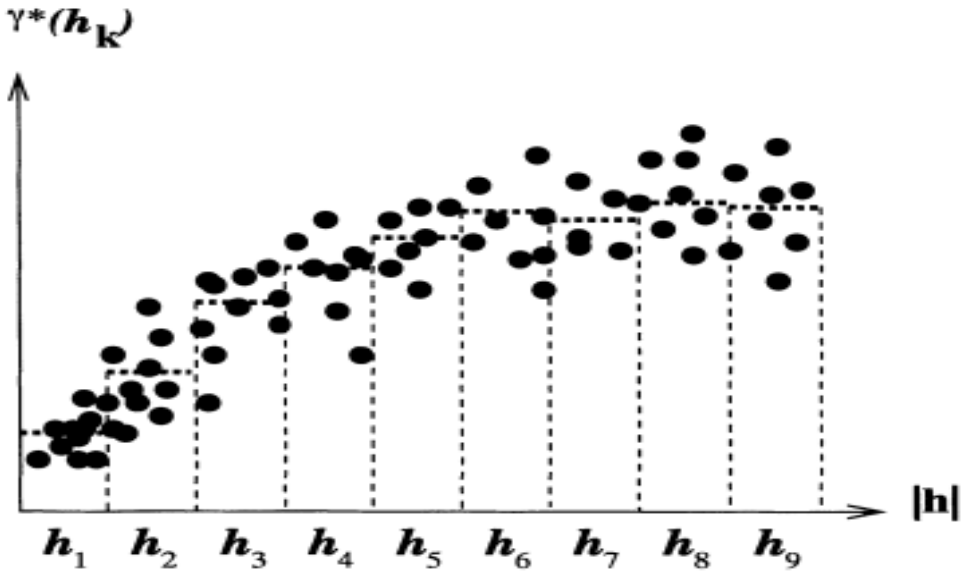


**Figure 2:** The experimental variogram. Source: Wackernagel (2003)**.**

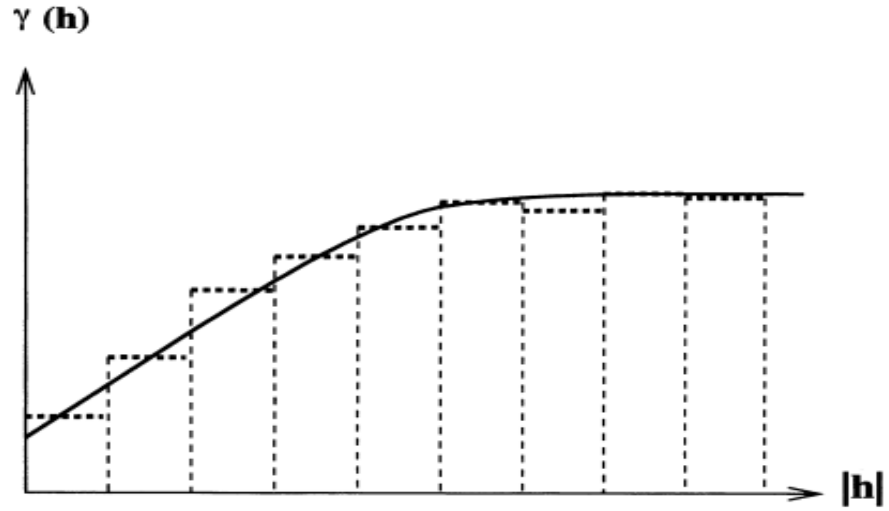


**Figure 3:** The sequence of average dissimilarities is fitted with theoretical variogram function. Source: Wackernagel (2003).

## 3. Result and Discussion

### 3.1 FLDAS Downward Longwave Radiation Data Validation

The LWD dataset obtained from the FLDAS model was validated using BSRN LWD observations the result shows FLDAS LWD and measured LWD has an RMSE value of 4.84, MAE value of 4.00, MBE value 0.2155 and a Pearson correlation value of 0.94. The high correlation between the two datasets and the low error magnitude suggests that the FLDAS LWD is reliable to be used for the generation of radiation map for Nigeria. FLDAS LWD underestimated the value of LWD in January, July, August, September, October, and December, while it overestimated LWD in April, May, June, and November (figure 4). The precise explanations for overestimation or underestimation of the FLDAS model over several months are beyond the reach of this analysis because a multi-year monthly average has been used and the existence of an outlier can contribute to the observed overestimation or underestimation.

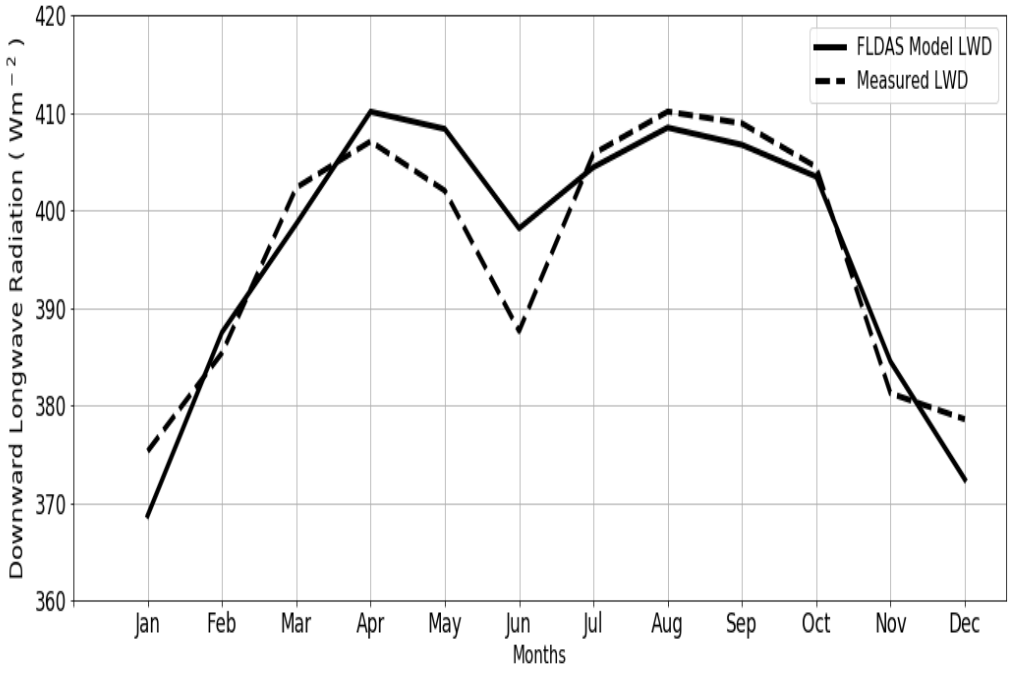


**Figure 4:** LWD dataset Validation.

### 3.2 Spatio-temporal Variations of LWD over Nigeria

The spatial variation of LWD was visualized using radiations map of Nigeria and variograms generated using the multi-year monthly average FLDAS LWD data.

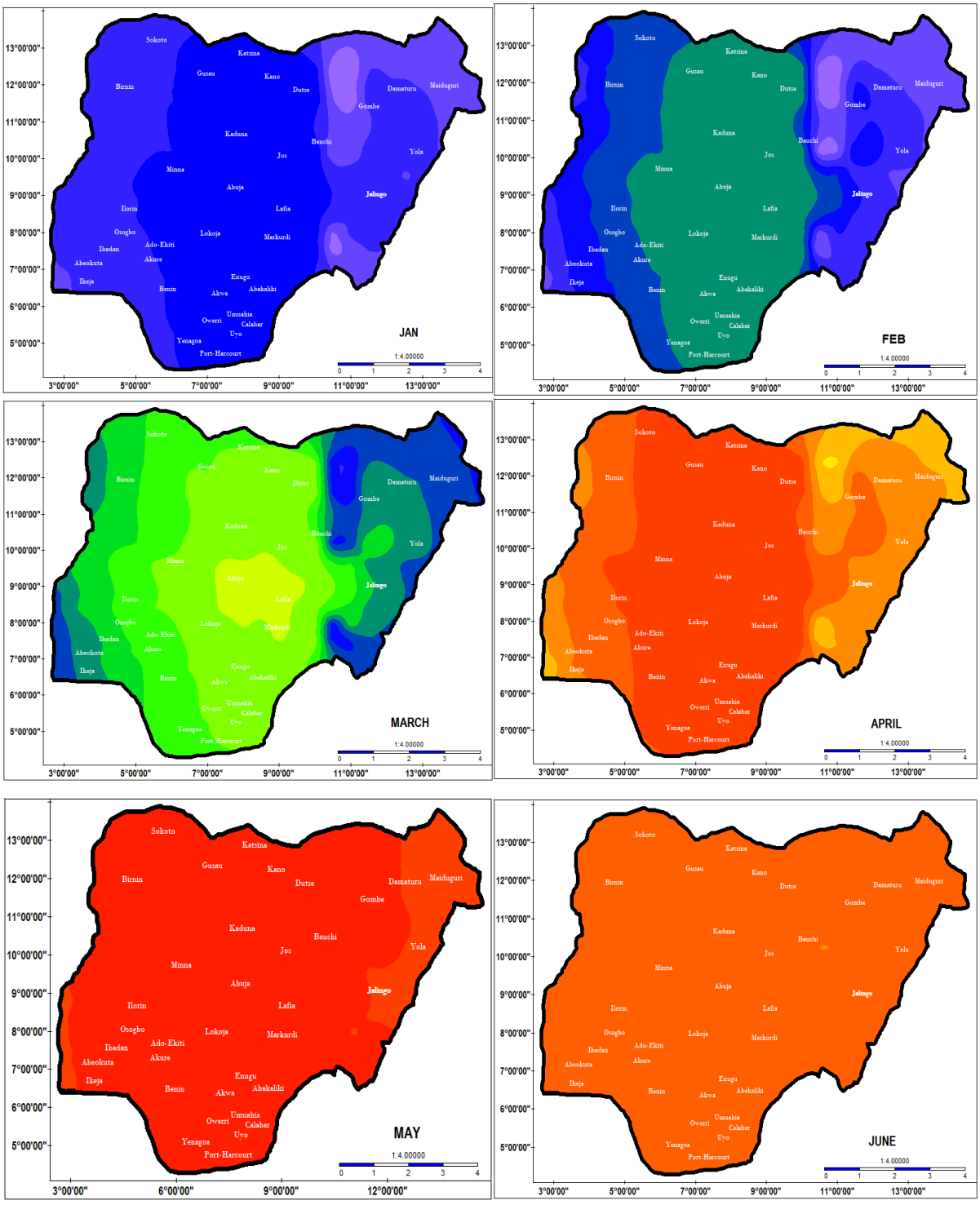
JAN
FEB
MARCH
APRIL
MAY
JUNE
Sokoto
Katsina
Gusau
Kano
Birnin
Dutse
Damaturu
Maiduguri
Gombe
Kaduna
Bauchi
Jos
Yola
Minna
Abuja
Jalingo
Ilorin
Lafia
Osogbo
Lokoja
Markurdi
Ibadan
Ado-Ekiti
Akure
Abeokuta
Ikeja
Benin
Enugu
Akwa
Abakaliki
Umuahia
Owerri
Calabar
Uyo
Yenagoa
Port-Harcourt
1:4.00000

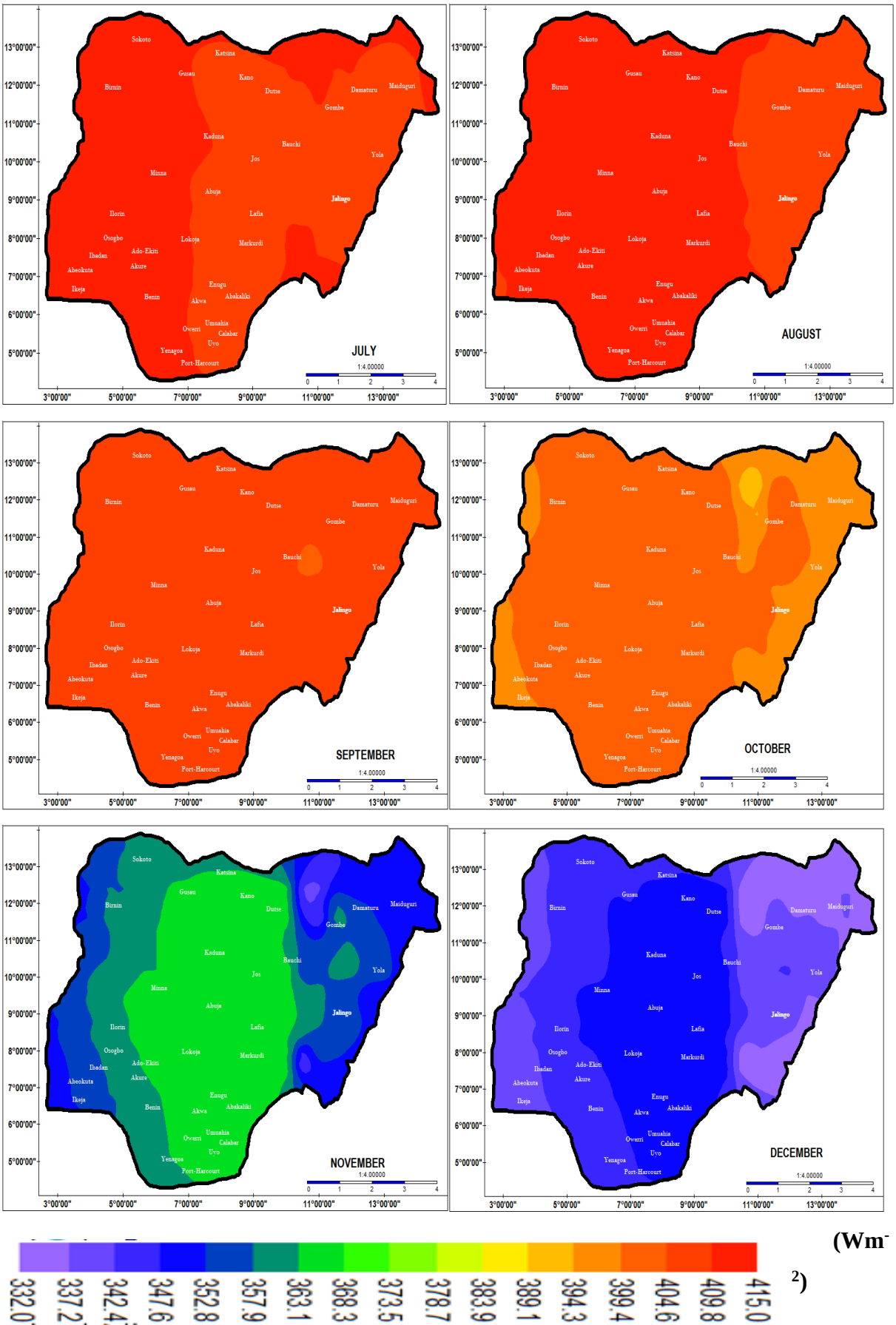
JULY
AUGUST
SEPTEMBER
OCTOBER
NOVEMBER
DECEMBER
(Wm-2)
332.0
337.2
342.4
347.6
352.8
357.9
363.1
368.3
373.5
378.7
383.9
389.1
394.3
399.4
404.6
409.8
415.0

**Figure 5:** Downward Longwave Radiation maps for Nigeria.

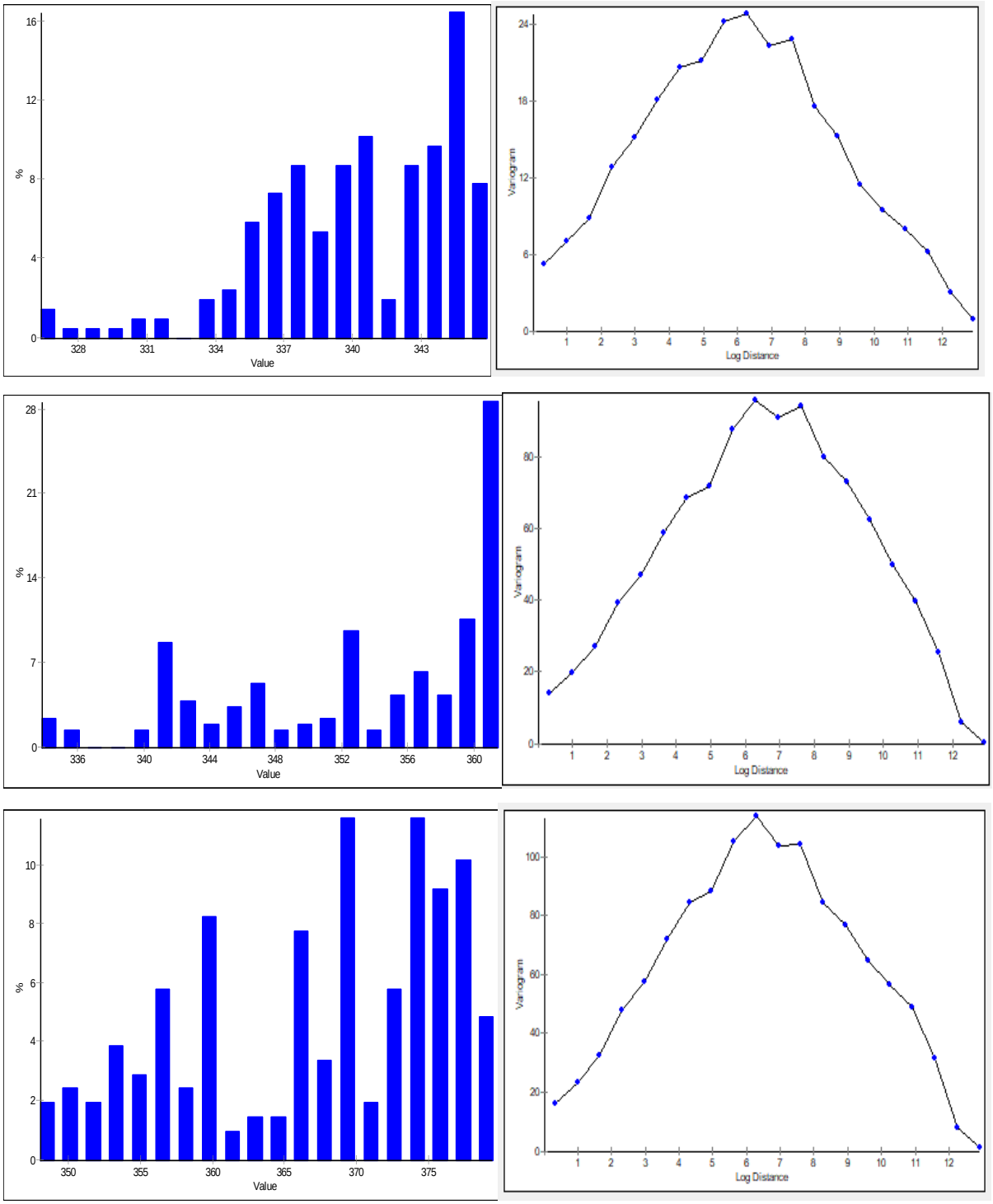

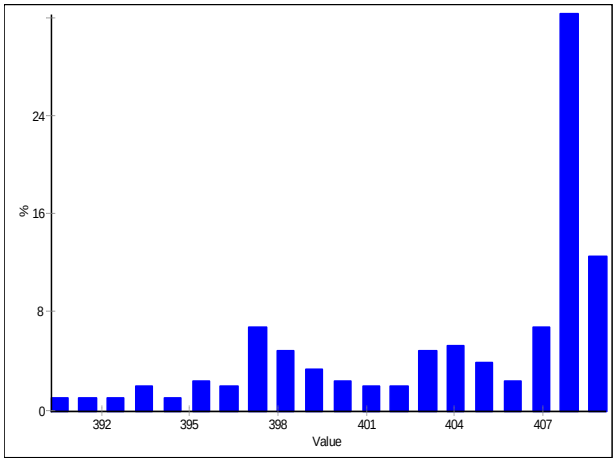
%
Value
392
395
398
401
404
407

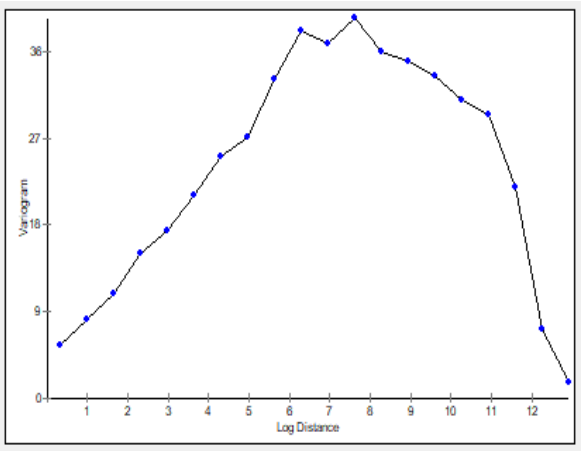
Variogram
Log Distance

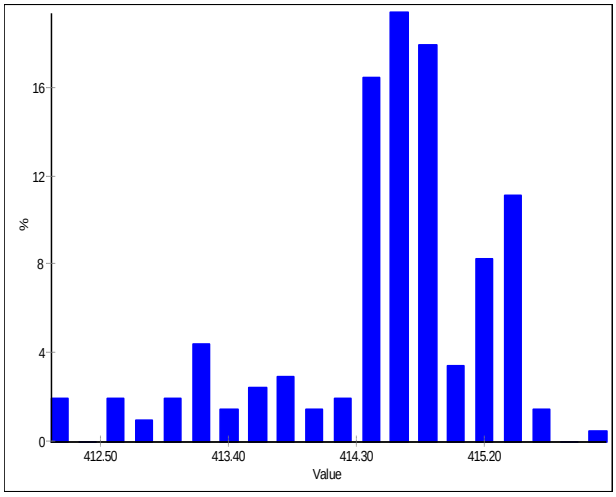
%
Value
412.50
413.40
414.30
415.20

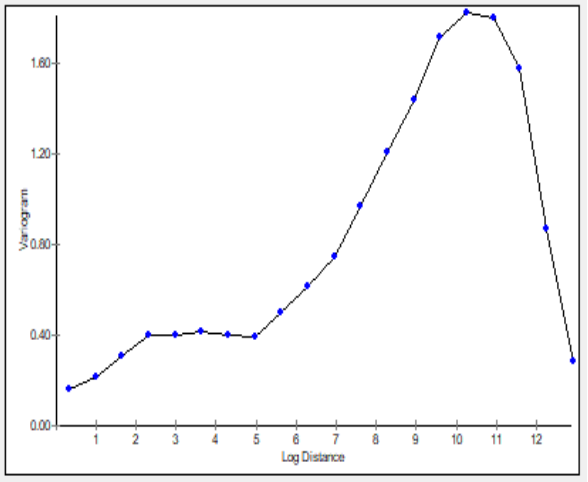
Variogram
Log Distance

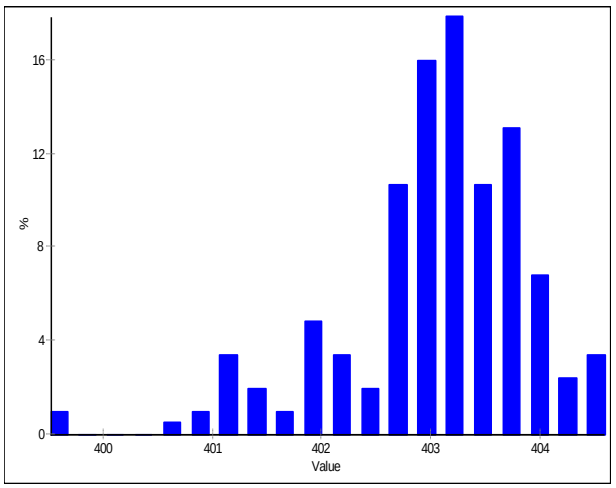
%
Value
400
401
402
403
404

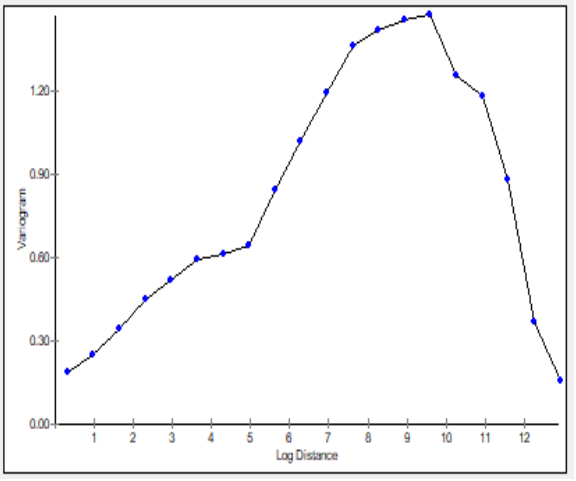
Variogram
Log Distance

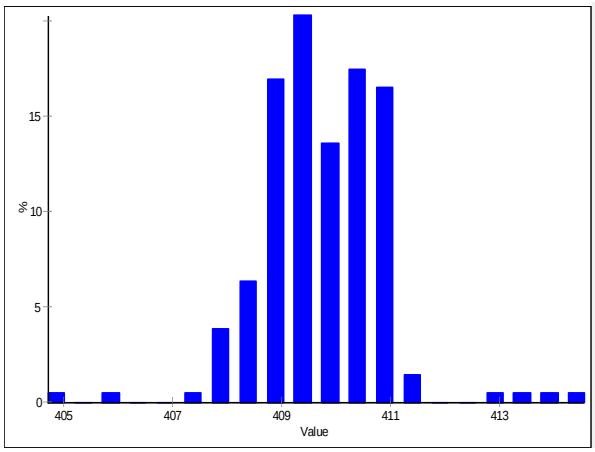
%
Value
405
407
409
411
413

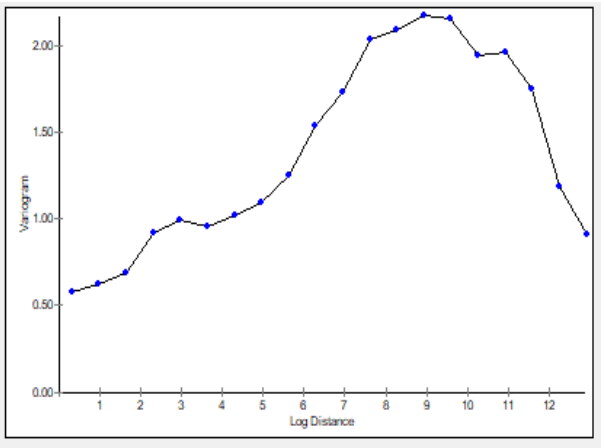
Variogram
Log Distance

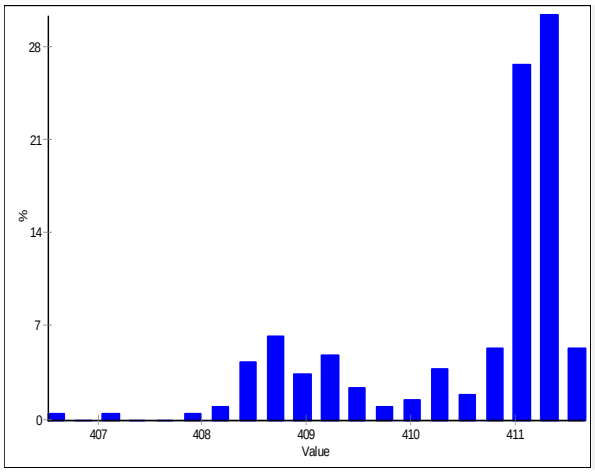
%
Value
407
408
409
410
411

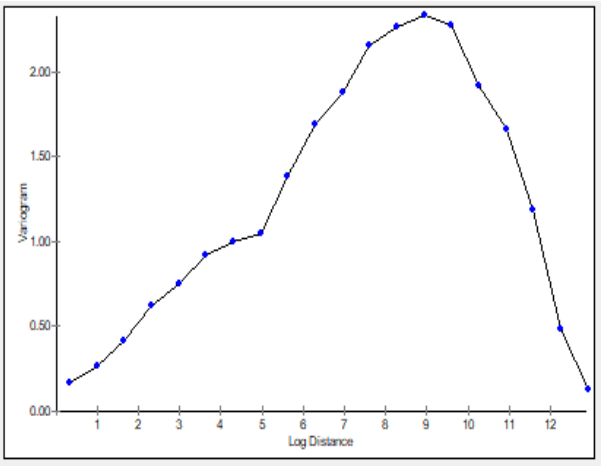
Variogram
Log Distance

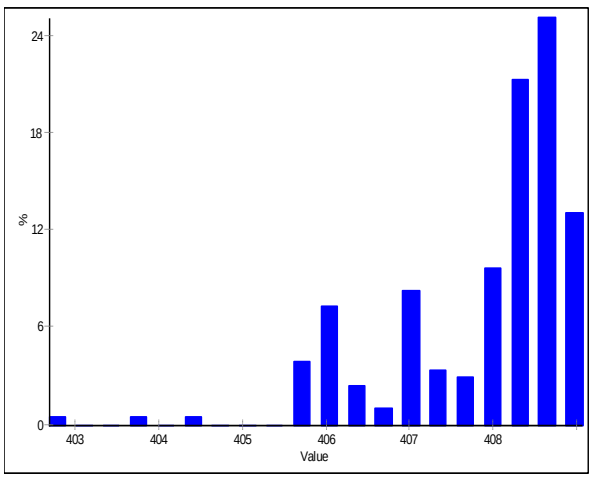
%
Value
403
404
405
406
407
408

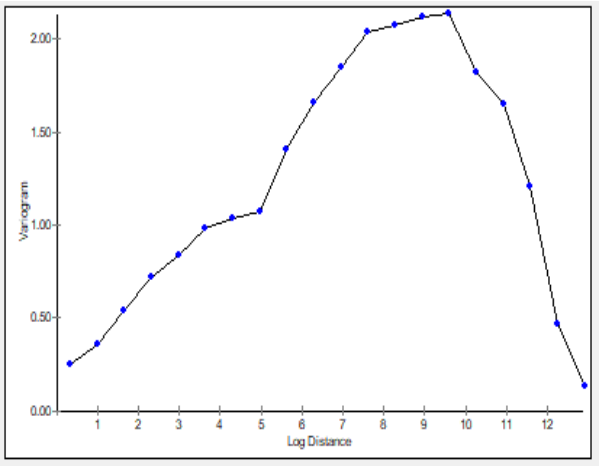
Variogram
Log Distance

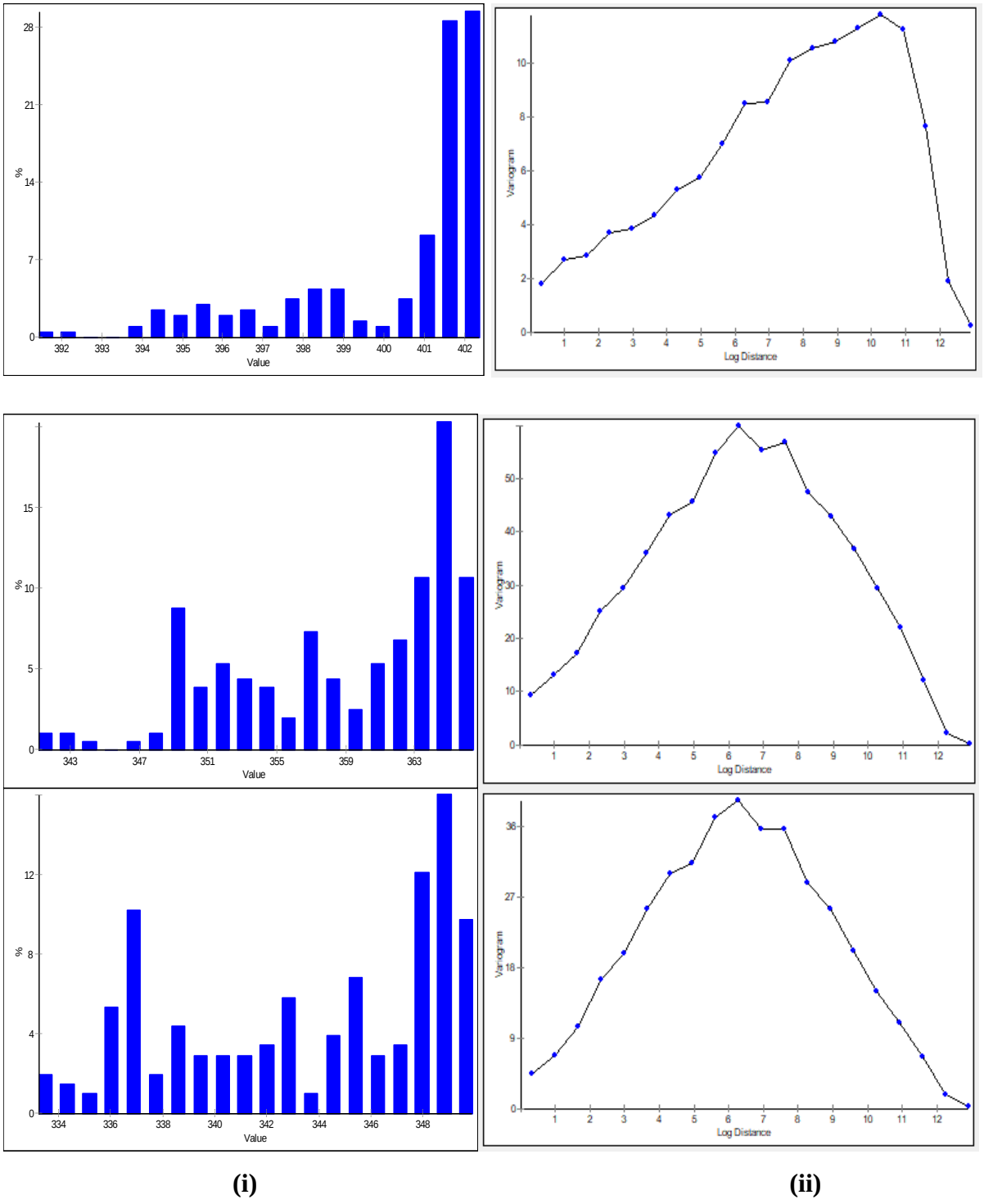


**Figure 6:** (i) Distribution of downward longwave radiation. (ii) Variogram of Downward Longwave Radiation (January to December from top to bottom).

The LWD radiation maps show the distribution of LWD over Nigeria for the twelve months in a calendar year (Figure 5). Table 1 shows the statistical summary of the LWD over Nigeria. The maximum, mean and minimum and STD LWD is the multi-year spatial

maximum, mean, minimum and standard deviation LWD over Nigeria for each month. The value of LWD across the sample space and time ranges from 332 $Wm^{-2}$ to 416 $Wm^{-2}$ with the extreme high LWD values appearing red and extreme low LWD values appearing in blue as indicated by the colour scale scheme (Figure 5). Variograms (Figure 6 (ii)) illustrate the spatial correlation of LWD over Nigeria from January to December. The shape of the variograms indicates that LWD values are similar at the two ends (west and east) but disparate at the central. The high dissimilarity values on the variogram and standard deviation (STD) show low spatial correlation or strong spatial variation in the distribution of LWD from November to March. LWD was observed to be higher around central Nigeria and lower around the west and east of Nigeria from November to March. The curve of the variograms is skewed towards the left from April to October indicating spatial correlation reduces from west to east of Nigeria. The low variogram values and STD during the aforementioned months indicate high spatial correlation or weak spatial variation in the distribution of LWD over Nigeria during these months. The distribution of LWD over Nigeria have a strong negative skew in February, April, August, September, October, very weak negative skew in March, November and December, and moderate skew in January and June. The distribution of LWD over Nigeria in May has a very weak negative skew, while the distribution in July is almost close to a normal distribution (Figure 6 (ii)).

The temporal variation of LWD over Nigeria is not even as indicated by the radiation maps i.e. the rate of change of LWD varies across locations. This can be due to variation in the spatial distribution of temperature, water vapour and other longwave radiation-emitting atmospheric particle. LWD suffered the maximum variation in the spatial distribution in March as indicated by the high standard deviation of 8.70, the minimum spatial variation in May as indicated by a STD of 0.75 and uniformity in the colour of radiation map for May. On the annual survey, LWD values in the rainy season (April to September) are higher (deeper red) than in the dry season. This is due to the high moisture content of the atmosphere and significantly high temperature compared to the dry season with low humidity and extreme cold and hot temperature, especially during harmattan. Furthermore, LWD has a very low spatial variation during rainy season compared to the dry season with higher variations as indicated by the high STD. This is due to the more uniform distribution of water vapour in the atmosphere during the rainy season compared to the dry season.

**Table 1:** Multi-year monthly data summary.

| Months | Max ($Wm^{-2}$) | Mean ($Wm^{-2}$) | Min ($Wm^{-2}$) | STD |
|---|---|---|---|---|
| 1 | 352.53 | 346.68 | 332.62 | 4.21 |
| 2 | 362.40 | 353.89 | 334.19 | 7.99 |
| 3 | 380.54 | 368.13 | 348.51 | 8.70 |
| 4 | 407.80 | 402.49 | 388.52 | 5.03 |
| 5 | 412.19 | 410.57 | 408.20 | 0.75 |
| 6 | 404.47 | 402.86 | 399.29 | 0.86 |
| 7 | 414.92 | 409.95 | 404.85 | 1.10 |
| 8 | 411.64 | 410.47 | 406.39 | 1.08 |
| 9 | 409.29 | 408.05 | 402.77 | 1.09 |
| 10 | 402.74 | 400.61 | 391.59 | 2.45 |
| 11 | 367.26 | 359.52 | 341.52 | 6.30 |
| 12 | 350.51 | 344.13 | 333.46 | 5.10 |

The seasonal variation of LWD is the effect of the revolution of the earth around the sun, leading to variation in insolation as sun angle changes, which directly and indirectly affects the amount of LWD. The direct effect is the variation in the level of shortwave radiation received in Nigeria and the indirect effect is the effect of insolation on the trade winds (The Tropical Continental airmass and the Tropical Maritime airmass) dictating the climate pattern of Nigeria. During the dry season, West Africa is laden with dust particles from Sahara Desert carried by the tropical continental airmass. These dust particles obstruct most of the incoming solar radiation thereby cooling the earth and reduces evapotranspiration thus creating a dry atmosphere consequently reducing the amount of LWD. The position of the sun in the atmosphere and oblique shape of the earth, cause variation in insolation across latitude leading to differential heating which consequently affects the spatial distribution of pressure on the earth's surface. This makes West Africa an area of low pressure around June when the sun is overhead at the equator, resulting in the withdrawal of the tropical continental airmass towards the northward and the movement of the tropical airmass which originates from the Atlantic Ocean towards the north, supplying the much-needed humidity. The movement of the air masses causing high relative humidity and movement of the earth causing hot temperature explains the seasonal variation of LWD over Nigeria and West Africa.

## 4. Conclusion

The Spatio-temporal variation of downward longwave radiation (LWD) was studied using FLDAS LWD dataset. The FLDAS LWD dataset was validated using ground-measured LWD data taken with a pyrgeometer. The two datasets compared well with an RMSE value of 4.84, MAE value of 4.00 and MBE value 0.2155. This shows that FLDAS LWD product can be used when and where ground-measured LWD data is not available. The results of this study indicate that the spatial variation of LWD is not uniform throughout the months and season of the year. Lower spatial variation was observed during rainy season as compared to the dry season and as indicated by the value of STD, variogram and radiation map with the largest variation in spatial data occurring in March and lowest variation occurring in May. Locations around the central part of Nigeria recorded highest LWD, which reduces eastward and westward during the dry season. Significantly higher LWD was observed during the rainy season in comparison with the dry season, Highest spatial average of 410.57 $Wm^{-2}$ recorded in May and lowest (344.13 $Wm^{-2}$) in December. The highest monthly average of 414.92 $Wm^{-2}$ was recorded in July and the lowest of 332.62 $Wm^{-2}$ was recorded in January. Spatial distribution of LWD which could not be studied with ground-measurements was successfully depicted. The LWD map developed in this study will be very useful for estimating LWD with a significant level of accuracy. It can also be used for LWD related study like; hydrological cycle, latent heat and energy balancing components.

**Acknowledgement**

The authors wish to appreciate the Goddard Earth Sciences (GES) Data and Information Services Center (DISC) for making the data used in this study available. We also acknowledge the anonymous reviewers for their contributions.

## References

Abramowitz, G., Pouyanne, L. and Ajami, H. (2012): On the information content of surface meteorology for downward atmospheric longwave radiation synthesis. *Geophysical Research Letters.* **39**, L04808.

Ångström, A. (1918): A study of the radiation of the atmosphere. *Smithsonian miscellaneous collections.* **65**, 1–159.

Aro, T. O. (2007): Basic measurements of radiation at station Ilorin (1992-12). *Department of Physics, University of Ilorin, PANGAEA, https://doi.org/10.1594/PANGAEA.669798.*

Brunt, D. (1932): Notes on radiation in the atmosphere. *Quarterly Journal of the Royal Meteorological Society*, **58**, 389–420.

Brutsaert, W. H. (1975): On a derivable formula for long-wave radiation from clear skies. *Water Resources Research*. **11**, 742–744.

Iacono, M. J., Delamere, J. S., Mlawer, E. J., Shephard, M. W., Clough, S. A. and Collins, W. D. (2008): Radiative forcing by long-lived greenhouse gases: Calculations with the AER radiative transfer models. *Journal of Geophysical Research: Atmosphere*, **113** D13103.

Idso, S. B. and Jackson, R. D. (1969): Thermal radiation from the atmosphere. *Journal of Geophysical Research*. **74**, 5397–5403.

Koike, T. (2004): The coordinated enhanced observing Period: An initial step for integrated global water cycle observation. *World Meteorological Organization Bulletin*. **53** (2), 115–121.

Lawford, R., *et al*. (2006): U.S. Contributions to the CEOP. *Bulletin of the American Meteorological Society*, **87** (7), 927–939.

McNally, A. *et al*. (2017): A land data assimilation system for sub-Saharan Africa food and water security applications. *Scientific Data*. **4**, 170012.

Mölders, N., Luijting, H. and Sassen, K. (2008): Use of atmospheric radiation measurement program data from Barrow, Alaska, for evaluation and development of snow albedo parameterizations. *Meteorology and Atmospheric Physics*. **99**, 199-219.

Ohmura, A., *et al*. (1998): Baseline Surface Radiation Network (BSRN/WCRP): New precision radiometry for climate research, *Bulletin of the American Meteorological Society*, **79** (10), 2115–2136.

Ryu, Y., Kang, S., Moon, S.K. and Kim, J. (2008): Evaluation of land surface radiation balance derived from moderate resolution imaging spectroradiometer (MODIS) over complex terrain and heterogeneous landscape on clear sky days. *Agricultural and Forest Meteorology*. **148**, 538-1552.

Sur, C., Kim, H. and Choi, M. (2014): Satellite-based downward longwave radiation measurement using various models in Northeast Asia. *Terrestrial, Atmospheric and Oceanic Sciences*. **25**, 893-902.

Swinbank, W. C. (1963): Long-wave radiation from clear skies. *Quarterly Journal of the Royal Meteorological Society*. **89**, 339–348.

Trenberth, K. E., Fasullo, J and Smith, L. (2005): Trends and variability in column-integrated atmospheric water vapour. *Climate Dynamics*. **24** (2), 440–454.

Trenberth, K. and Fasullo, J. (2012): Tracking Earth's energy: From El Niño to global warming. *Surveys in Geo-physics*. **33** (3), 413–428.

Wackernagel, H. (2003): *Multivariate Geostatistics: An Introduction with Applications*. 3rd ed. Springer, Heidelberg.

Wang, K. C. and Liang, S. (2009): Global atmospheric downward longwave radiation over land surface under all-sky conditions from 1973 to 2008. *Journal of Geophysical Research*. **114**, D19101.

**Data Availability:** The data used in this study are available at the BSRN Pangea portal (https://www.pangaea.de) and the "NASA earthdata" portal (https://giovanni.gsfc.nasa.gov).